

Propagation of sound in a Bose Einstein condensate in an optical lattice

C. Menotti¹, M. Krämer¹, A. Smerzi^{1,2}, L. Pitaevskii^{1,3}, and S. Stringari¹

¹*Istituto Nazionale per la Fisica della Materia BEC-CRS and Dipartimento di Fisica, Università di Trento, I-38050 Povo, Italy*

²*Theoretical Division, Los Alamos National Laboratory, Los Alamos, NM 87545, USA*

³*Kapitza Institute for Physical Problems, 117334 Moscow, Russia*

(Dated: September 28, 2018)

We study the propagation of sound waves in a Bose-Einstein condensate trapped in a one-dimensional optical lattice. We find that the velocity of propagation of sound wavepackets decreases with increasing optical lattice depth, as predicted by the Bogoliubov theory. The strong interplay between nonlinearities and the periodicity of the external potential raise new phenomena which are not present in the uniform case. Shock waves, for instance, can propagate slower than sound waves, due to the negative curvature of the dispersion relation. Moreover, nonlinear corrections to the Bogoliubov theory appear to be important even with very small density perturbations, inducing a saturation on the amplitude of the sound signal.

The study of Bose Einstein condensates in optical lattices is a very active field of research, both from the theoretical and experimental sides. The presence of the lattice can dramatically modify the behaviour of the system with respect to the uniform case, giving rise to new phenomena like, for instance, a Mott-insulator superfluid phase transition [1, 2] or the occurrence of dynamical instabilities [3, 4, 5, 6, 7, 8]. Several efforts are also focusing on the creation of quantum computers [9] and ultrasensitive interferometers [10]. In this paper we study the propagation of sound waves on top of a Bose-Einstein condensate at rest in a one-dimensional lattice.

The propagation of sound in a harmonically trapped condensate without lattice has been already observed experimentally [11, 12] and studied theoretically [13, 14, 15, 16]. Generally speaking, it is important to study the propagation of sound also in the non linear regime, where density fluctuations are comparable to the background density of the condensate. The reason is that only large amplitude wavepackets can be realistically observed experimentally. It turns out, however, that nonlinear effects in the sound propagation are particularly interesting also from the theoretical point of view. For instance, the formation of shock waves in front of a bright sound wavepacket (positive density variation) a uniform or harmonically trapped condensates has been studied in [16], and analytical solutions have also been discussed in [17, 18, 19]. In the presence of a periodic potential, theoretical aspects of the propagation of sound have been so far explored only in the linear regime [5, 20, 21, 22, 23, 24, 25, 26, 27, 28, 29, 30]. The main question addressed in this work is the strong interplay between nonlinear effects and the periodicity of the external potential.

We assume a fully coherent condensate described by an effective one-dimensional Gross-Pitaevskii (GP) equation. In the uniform case, the spectrum of elementary excitations is given by the well-known Bogoliubov dispersion relation $\omega(q) = \sqrt{q^2/2m(q^2/2m + 2U)}$, where q is the momentum of the excitation, m the atomic mass and $U = gn$ the inverse compressibility with $g = 4\pi\hbar^2 a/m$ the interaction strength and n the density. For momenta q smaller than the inverse of the healing length

$\xi = 1/\sqrt{8\pi an}$, the excitation spectrum depends linearly on the momentum with a slope $c = \sqrt{U/m}$ which defines the sound velocity.

We now consider a condensate in a one dimensional optical lattice

$$V_{opt}(x) = s E_R \sin^2\left(\frac{\pi x}{d}\right), \quad (1)$$

characterized by a lattice spacing d and a depth s in units of the recoil energy $E_R = \hbar^2\pi^2/2md$. The elementary excitations of a condensate in presence of a one dimensional lattice have been discussed in detail, e.g., in [29]. One of the main features is the formation of a band structure in the Bogoliubov spectrum when the lattice is turned on, in analogy with the linear Bloch theory. The spectrum is periodic in the quasi-momentum q of the excitations and, for a given q , many excitation energies, labeled by a band index, are available. Energy gaps open at the boundary and at the center of the Brillouin zone, given respectively by the Bragg momentum $q_B = \hbar\pi/d$ and $q_B = 0$.

As in the uniform case, the energy of low energy excitations is linear in the quasi-momentum, $\hbar\omega = c|q|$, and the system admits sound waves with velocity

$$c = \sqrt{\frac{U}{m^*}}. \quad (2)$$

The inverse compressibility U increases very weakly with the optical lattice depth s , and the effective mass m^* instead strongly increases with s , reflecting the corresponding quenching of the tunneling rate through the barriers. As a consequence the sound velocity is predicted to decrease for increasing lattice depth. In the tight binding limit, the effective mass is related to the tunneling parameter δ by $m^*/m = 2E_R/(\pi^2\delta)$ and the sound velocity can thus be written as $c = d\sqrt{U\delta}/\hbar$ [28, 29].

However, it is not obvious whether a sound signal of observable amplitude can propagate also in deep lattices, where the tunneling rate is very small and nonlinear corrections to the Bogoliubov theory can be important. For instance, nonlinear effects combined with the presence of periodic trapping potentials dramatically affect the center-of-mass motion of harmonically driven condensates due to the onset of dynamical instabilities [4, 5, 6].

This paper is organized as follows: In Sect. I, we outline the procedure to generate a sound signals. In Sect. II we introduce our theoretical analysis, based on both the Gross-Pitaevskii (GP) equation and the discrete nonlinear Schrödinger equation (DNLS). In Sect. III we obtain the velocity of propagation of large amplitude wavepackets, and in Sect. IV we discuss the different regimes for sound propagation. In Sect. V we comment on the consequences of an additional harmonic trapping and, finally, in Sect. VI we conclude discussing the experimental observability of the predicted effects.

I. GENERATION OF SOUND SIGNALS

One possibility to create excitations in the condensate consists in turning on and/or off a perturbation potential in the center of the system, for instance by means of a far detuned laser beam. If the width of the perturbing potential is much larger than the lattice spacing, only quasi-momenta much smaller than the Bragg momentum q_B are addressed. This procedure generates a pair of wavepackets propagating symmetrically outwards. Moreover, only Bogoliubov bands with energy lower than the inverse time scale T_p of the perturbation are excited. In particular, since the gap between first and second Bogoliubov band at the center of the Brillouin zone is of the order of $4E_R$, one has multiple-band excitations if $T_p < \hbar/4E_R$, otherwise if $T_p \gg \hbar/4E_R$ only the lowest band is addressed. The result of a fast perturbation ($T_p = \hbar/E_R$) at low lattice depth is shown in Fig.1. One finds two pairs of wavepackets propagating at two different velocities. The velocity of the slower ones is given by the sound velocity (2), while the velocity of the faster ones is given approximatively by $2q_B/m$, close to the derivative of the second and third band of the spectrum at small q . Those fast wavepackets are not sound waves but are superpositions of single particle excitations: they disappear in absence of the lattice, but if the lattice is present they are found in a non-interacting gas as well. Apparently, they travel without changing shape, simply because the curvature of the spectrum is too small to observe their dispersion on the time scale of our simulation. This effect can be observed only in presence of shallow lattices, when the gap between second and third band is negligible. For larger s , such single particle excitations travel with smaller velocity, disperse more quickly, and can interfere with the propagation of the sound wavepackets. For this reason it is better to use slower perturbations $T_p \gg 1$ in order to restrict the dynamics to the first band.

The shape of the wavepackets depends on the excitation procedure. However, the main features of their behaviour are quite general. In absence of the lattice, the observation of sound signals in a harmonically trapped condensate was achieved experimentally by employing

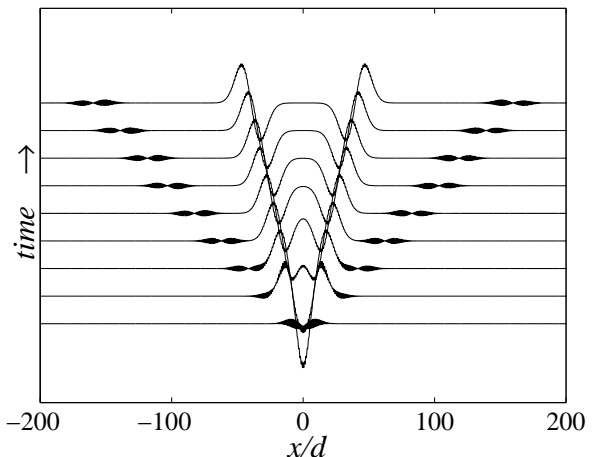


FIG. 1: GP simulation of wavepackets produced by a fast ($T_p = 1$) perturbation of the type (3) in presence of an optical lattice ($s = 1$, $gn = 0.5E_R$). Both the first, the second and the third bands are excited leading to the formation of two pairs of wavepackets. For a slow perturbation ($T_p \gg 1$) only the slow pair composed of phonons of the lowest band is created. Here, we plot the relative density $n(x, t)/n(t, 0)$ as defined in Sect.II

two different excitations methods [11]: raising a potential barrier in the center of the trap produces a density bump, which splits into two *bright* sound wavepackets; alternatively, removing a potential barrier from the center of the condensate gives rise to a dip in the density which splits into two *grey* sound wavepackets.

The excitation method we adopt here is a combination of these two: The initial condensate is in the ground state of a one-dimensional optical lattice. We then switch on and off a gaussian potential in the center and get two composed *bright-grey* sound signals propagating symmetrically outwards. This procedure has the advantage that the ground states of the initial and final potential are identical.

The perturbing potential has a spatial and temporal dependence

$$V_P(x, t) = V_{Px}(x)V_{Pt}(t), \quad (3)$$

where

$$V_{Px}(x) = bE_R \exp[-x^2/(wd)^2], \quad (4)$$

$$V_{Pt}(t) = \begin{cases} 0, & \text{for } t < 0, \\ \sin^4\left(\frac{\pi E_R t}{\hbar T_p}\right), & \text{for } 0 < t < T_p \hbar/E_R \\ 0, & \text{for } t > T_p \hbar/E_R. \end{cases} \quad (5)$$

The tunable dimensionless parameters are the width of the potential w , its height b and the time of perturbation T_p . We impose the constraints

$$w \gg 1, \quad (6)$$

in order to address only the quasi-momenta in the central part of the Brillouin zone, and

$$T_p > 1 \quad (7)$$

in order to excite the lowest Bogoliubov band only. Note that for typical densities, scattering lengths and lattice spacings, ξ is of the order of d . Hence, $w \gg 1$ automatically implies $wd \gg \xi$, which ensures that the produced excitations are phonons.

II. GROSS-PITAEVSKII (GP) AND DISCRETE NONLINEAR SCHRÖDINGER EQUATIONS (DNLS)

We study the sound propagation in the presence of the lattice potential (1) with the one-dimensional GP-equation

$$i\hbar\dot{\varphi} = \left[-\frac{\hbar^2 \partial_x^2}{2m} + V(x,t) + gnd|\varphi(x,t)|^2 \right] \varphi(x,t), \quad (8)$$

describing a system uniform in the transverse directions y, z with n the 3D average density. The consequences of a transverse confinement, which can modify the degree of nonlinearity of the system and the speed of sound [28], are discussed in Sect.V. The normalization of the wavefunction is $\int_{-N_w d/2}^{N_w d/2} |\varphi(x,t)|^2 dx = N_w$, with N_w the total number of lattice wells. The external potential $V(x,t)$ is given by the sum of the lattice potential $V_{opt} = sE_R \sin^2(\pi x/d)$ and the time-dependent perturbation $V_P(x,t)$ written in Eq.(3)

$$V(x,t) = V_{opt}(x) + V_P(x,t). \quad (9)$$

The ground state of the system in the presence of the optical potential is governed by two parameters: the optical lattice depth s and the interaction strength gn .

Writing $\varphi(x,t) = \sqrt{n(x,t)/n} \exp[iS(x,t)]$, the GP-equation (8) can be recast in the form of two coupled equations for the density and phase variables

$$\begin{aligned} \dot{n}(x) &= -\partial_x \left[n(x) \frac{\hbar}{m} \partial_x S(x) \right], \\ \dot{S}(x) &= -\frac{1}{\hbar} [V(x,t) + gn(x) + \\ &\quad -\frac{\hbar^2}{2m\sqrt{n}} \partial_x^2 \sqrt{n} + \frac{\hbar^2}{2m} (\partial_x S(x))^2]. \end{aligned} \quad (10)$$

In the presence of the lattice, both the density and the phase are characterised by very strong modulations on the length scale of the lattice spacing d . In order to highlight the density variation corresponding to the sound wavepacket, it is in general convenient to plot the density relative to the ground state density $n(x,t)/n(x,0)$. Alternatively, in order to mimic the limited resolution of a detection system, one can perform a convolution over a few lattice wells of the GP results for $n(x,t)$. We also consider the evolution of the relative phase between neighboring wells, defined as

$$\phi_{\ell+1/2} = S(x = (\ell+1)d) - S(x = \ell d). \quad (11)$$

The typical signals obtained in a GP simulation in the linear regime are shown in Fig.(2), where in the upper panel we plot both the relative density $n(x,t)/n(x,0)$ and the convoluted signal. We denote by Δn and $\Delta\phi$ the signal amplitudes of the density and relative phase wavepackets respectively.

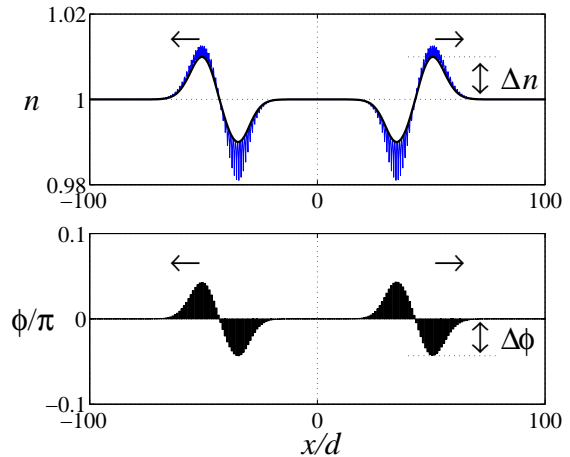


FIG. 2: Typical result of a GP simulation for small perturbations (linear regime). Two sound packets move symmetrically outward at the Bogoliubov sound velocity. The relative density $n(x,t)/n(x,0)$ (thin line), the convoluted signal (thick line) and the phase difference $\phi_{\ell+1/2}$ are shown. The signal amplitudes of the density and relative phase are denoted by Δn and $\Delta\phi$ respectively.

In the tight binding regime, where the condensate phase is approximately flat in each well, the GP dynamics can be simplified by using the discretised wavefunction $\psi_\ell = \sqrt{n_\ell(t)} \exp[iS_\ell(t)]$, where $n_\ell(t) = |\psi_\ell(t)|^2 = \int_{\ell d - d/2}^{\ell d + d/2} |\varphi(x,t)|^2 dx$ and $S_\ell(t) = S(x = \ell d, t)$. At equilibrium $n_\ell = 1$ and $S_\ell = 0$. The time evolution of ψ_ℓ is given by the discrete nonlinear Schrödinger equation (DNLS) [31]

$$i\hbar\dot{\psi}_\ell = -\frac{\delta}{2} (\psi_{\ell+1} + \psi_{\ell-1}) + [V_\ell(t) + U|\psi_\ell(t)|^2] \psi_\ell(t). \quad (12)$$

Here, the external potential $V_\ell(t)$ includes only the perturbation $V_P(\ell d, t)$, with V_P given by (3), since the presence of the optical lattice potential is accounted for by the discretization of space. The two quantities δ and U entering the DNLS describe, respectively, the tunneling coupling between two neighbouring wells (corresponding to half the height of the lowest Bloch band) and the on-site interaction U (corresponding to the inverse compressibility).

In terms of density and phase variables, the DNLS equation becomes

$$\dot{n}_\ell = \sum_{\ell'=\ell\pm 1} \frac{\delta}{\hbar} \sqrt{n_\ell(t)n_{\ell'}(t)} \sin[S_\ell(t) - S_{\ell'}(t)], \quad (13)$$

$$\dot{S}_\ell = -\frac{\mu_\ell}{\hbar} + \sum_{\ell'=\ell\pm 1} \frac{\delta}{2\hbar} \sqrt{\frac{n_{\ell'}(t)}{n_\ell(t)}} \cos[S_\ell(t) - S_{\ell'}(t)],$$

where $\mu_\ell = Un_\ell + V_\ell$.

The results of the numerical integration of the DNLS equation (12) match those obtained by solving the GP-equation (8) in deep lattices. In order to compare the density $n(x,t)$ calculated with the GP equation with the solution $n_\ell(t)$ of the DNLS equation, it is necessary to average $n(x,t)$ over each lattice site. Instead the comparison for the evolution of the relative phase $\phi_{\ell+1/2} = S_{\ell+1} - S_\ell$ is straightforward.

The DNLS approach is not only convenient from the numerical point of view, but also allows a clearer and semi-analytical understanding of the basic physics underlying sound propagation and shock-waves formation in the tight binding regime. In particular the DNLS equation written in the form (13) is particularly useful to get insight into the breakdown of the linear regime for deep lattices (see discussion in Sect.IV).

In the following, we will discuss the solution of the GP-equation (8) and DNLS equation (12) for various values of the potential height b , the potential width w and the perturbation time T_p . We will vary the parameters s and gn in the case of the GP equation and the parameters δ and U in the case of the DNLS to explore different regimes of lattice depths and interaction strengths.

III. VELOCITY OF PROPAGATION OF WAVEPACKETS

The first quantity we want to extract from our simulations is the velocity of propagation of sound wavepackets as a function of lattice depth. The result in the linear regime has already been predicted in [29]. Here we focus on the case of large perturbations producing signals which can be observed experimentally.

In Fig. 3 we plot some examples for the relative density at the final stage of our GP-simulation at lattice depths $s = 0, 10, 20$ with $gn = 0.5E_R$ for a large perturbation. Those signals involve significant nonlinear effects, even in the uniform case (see Fig.3(a)). From these simulations, after performing the convolution of the signal, we obtain the sound velocity shown by the circles in Fig. 4. The respective signal amplitudes Δn , together with the Bogoliubov prediction (solid line) are also indicated in the figure.

The first conclusion is that from our simulation we can extract the value of the Bogoliubov sound velocity with high accuracy. Moreover, we find that sound signals of measurable amplitude can be observed also in deep lattices where the sound velocity is considerably lower than in the uniform system. At this value of gn , relatively large signal amplitudes can be obtained up to $s = 20$.

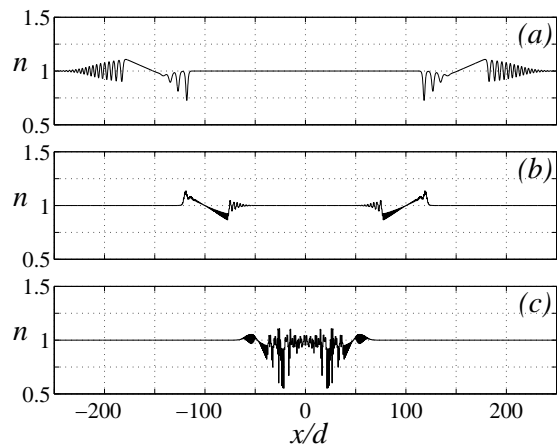


FIG. 3: GP simulation for the relative density $n(x,t)/n(x,0)$ at $t = 480\hbar/E_R$ with $gn = 0.5E_R$ for different lattice depths: $s = 0$ (a), $s = 10$ (b) and $s = 20$ (c).

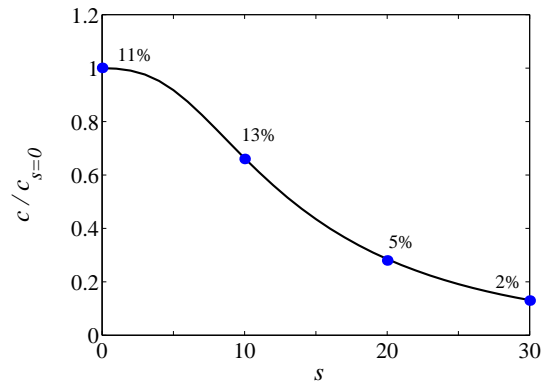


FIG. 4: Sound velocity as a function of lattice depth s . Bogoliubov prediction (solid line) and results “measured” based on the simulation (circles) with respective signal amplitudes Δn for $gn = 0.5E_R$. The signal amplitude Δn is defined as indicated in Fig. 2.

Note that the signal amplitudes obtained from the simulation at $s = 20, 30$ correspond to their saturated values as discussed in detail further below.

IV. LINEAR AND NONLINEAR REGIMES

By keeping lattice depth and interaction fixed while increasing the strength of the external perturbation, the role of nonlinearities becomes more and more important. The system passes through three regimes:

1. linear regime, where the Bogoliubov description holds and the variations of density and relative phases are small;
2. shock wave regime, where density variations induce mode-coupling among Bogoliubov excitations, giv-

ing rise to the formation of shock waves. Depending on the curvature of the Bogoliubov dispersion beyond the phononic regime, shock waves emerge in front of the wavepacket (uniform system, shallow lattice), both in the front and in the back (intermediate lattice) or only in the back (deep lattice with $\delta \ll U/3$). In the first two cases, the sound signal is deformed and it is finally dispersed. Instead, when shock waves form only in the back, the signal maintains a compact shape and propagates at the sound velocity predicted by Bogoliubov theory.

3. Saturation regime, where the sound signal amplitude saturates. The sound wavepacket leaves behind a wake of noise, and still propagates at the sound velocity predicted by Bogoliubov theory. This regime exists only in the presence of the lattice and provided that $\delta \ll U/3$ to ensure that shock waves form in the back of the signal as explained in regime (2). For fixed gn or U , the condition $\delta \ll U/3$ can be ensured by making the lattice sufficiently deep.

The signal amplitudes attainable in each regime and the perturbation parameters b , w , T_p needed to reach a certain regime depend on the lattice depth s and on the interaction strength gn , or equivalently, on δ and U . In the presence of a lattice, a stronger perturbation is needed to obtain the same signal amplitude as in absence of lattice. This reflects the fact that the condensate in a lattice is less compressible. In the following subsections we are going to discuss more in detail the three regimes.

1. Linear Regime

In the linear regime, the signal moves without dispersion and with sound velocity predicted by the Bogoliubov theory. The amplitudes Δn and $\Delta\phi$ are small and remain constant during the propagation. The ratio between the relative density and the relative phase amplitudes can be derived analytically. This can be done using the DNLS equations (13) valid only for deep lattices, or the macroscopic hydrodynamic formalism developed in [29] valid for all lattice depths and small quasimomentum.

A solution is provided by the ansatz

$$\bar{n}(x, t) = 1 + \Delta n[f_+(x - ct) + f_-(x + ct)], \quad (14)$$

$$\phi(x, t) = -\Delta\phi[f_+(x - ct) - f_-(x + ct)], \quad (15)$$

where \bar{n} represent either the DNLS density or the macroscopic averaged density. The functions f_+ and f_- describe respectively the wavepackets moving to the left and to the right, and Δn and $\Delta\phi$ are their amplitudes, as shown in Fig.2. We obtain

$$\Delta n = \frac{\hbar}{d} \sqrt{\frac{1}{Um^*}} \Delta\phi \xrightarrow{\text{DNLS}} \sqrt{\frac{\delta}{U}} \Delta\phi, \quad (16)$$

where the last expression is written in terms of DNLS parameters. We notice that in order to get the DNLS

relation, we have replaced $\sin[S_\ell(t) - S_{\ell'}(t)]$ with its argument, which implies $S_\ell(t) - S_{\ell'}(t) \ll \pi$. When this condition is not satisfied, non linear effects due to the optical lattice becomes important, and the linearised formalism breaks down.

2. Shock Wave Regime

The peculiarity of this region is the formation of shock waves. In the uniform case, a front wave emits shock waves in the forward direction (see Fig.3(a)). The stronger is the external perturbation, the stronger is the deformation and spreading of the sound wavepacket due to the emission of shock waves. We smoothen out the large density fluctuations in the shock wave region with a gaussian convolution of the signal over few lattice sites, mimicking the limited resolution of a detection system. A measurement of the position of maximum or the minimum of the resulting signal, propagating, respectively, faster and slower than sound, yields a velocity which deviates from the Bogoliubov prediction. However, in spite of the deformation of the signal, it is possible to extract the Bogoliubov value of the sound velocity as shown in Fig.4, by following the center-of-mass position of the signal [32].

In a shallow lattice, shock waves form in the front as in the uniform case, because the formation of a gap in the Bogoliubov spectrum does affect only a small range of quasi-momenta close to the Brillouin zone boundary. Hence, the mode-coupling among Bogoliubov excitations leads to the creation of excitations outside the phononic regime which travel at a speed larger than the sound velocity.

On the other hand, in intermediate and deep lattices shock waves can also form behind the sound packet due to the behaviour of the lowest band Bogoliubov dispersion, which in the tight binding regime takes the form [21, 29]

$$\hbar\omega_q \approx \sqrt{2\delta\sin^2\left(\frac{\pi q}{2q_B}\right) \left[2\delta\sin^2\left(\frac{\pi q}{2q_B}\right) + 2U\right]}. \quad (17)$$

For typical values of the density, the ratio δ/U lies between zero and one. If the ratio δ/U is larger than 1/3, the Bogoliubov dispersion has a positive curvature in a small range of quasimomenta and becomes negative closer to the zone boundary. In this case the shock waves are produced both in the front and in the back of the sound wavepacket. The dispersion has a negative curvature for all q as long as $\delta/U < 1/3$. In deep lattices (where $\delta/U \ll 1/3$), wavepackets composed by quasi-momenta outside the phononic regime will propagate much slower than sound and shock waves are therefore created behind the sound wavepacket (Fig.3(b) and Fig.5). In our simulations, for $\delta/U = 10^{-2}$, we observe that the relative phase distribution is strongly deformed if $\phi_{\ell+1/2} \sim \pi/2$, due to the non trivial sin-dependence of the current in the DNLS Eq.(13) (see Fig. 5 (upper two panels)). However this behaviour does not become

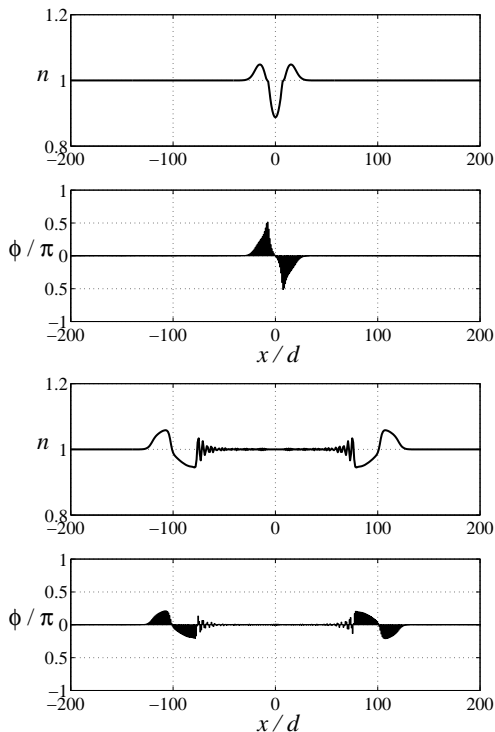


FIG. 5: DNL simulation of the density $n\ell(t)$ and relative phase $\phi_{\ell+1/2}$ for a deep lattice ($\delta/U = 10^{-2}$) in the shock wave regime ($T_p b/w \sim 5.5$). Upper panels: early stage ($t = 16\hbar/E_R$); lower panels: late stage ($t = 200\hbar/E_R$).

critical up to the point where the relative phase of two neighboring lattice sites $\phi_{\ell+1/2} = \pi$, which defines the onset of regime (3).

3. Saturation Regime in deep lattices

If we further increase the strength of the external perturbation, the relative phase $\phi_{\ell+1/2}$ at some site reaches π (see Fig.6, upper two panels) and there the current starts flowing in the opposite direction (see Eq.(13)). As a consequence, a wake of noise is left behind the sound packets and we find a saturation in the amplitude of the propagating signal (see Fig.3(c) and Fig.6, lower two panels). The interesting feature is that the noise has zero average velocity, since the oscillations of population between different wells are completely dephased. Provided that the lattice is deep enough to satisfy $\delta \ll U/3$, shock waves form only in the back of the signal, as discussed above. Hence the noise and the shock waves never overtake the sound signal, which is always able to “escape” from them.

We stress that this effect appears only in presence of a deep lattice. In fact, in the uniform case, even in presence of strong nonlinearities leading to a strong deformation of the signal, in the central region the system is always able to recover its ground state after the sound wave has passed by (see Fig.3 (a)).

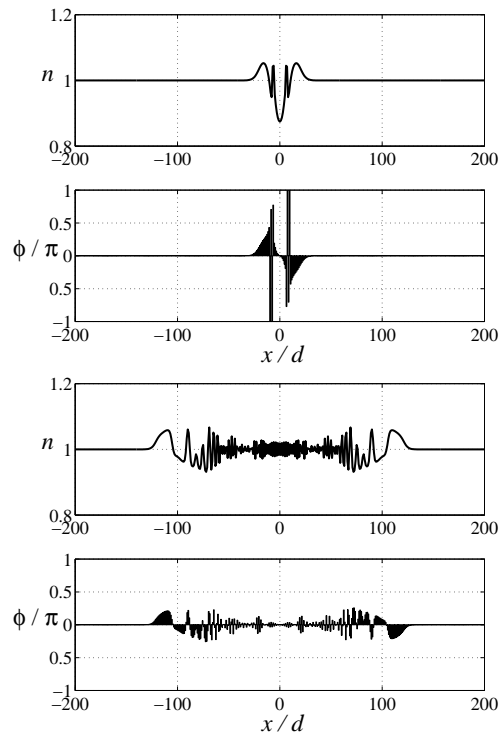


FIG. 6: DNL simulation of the density $n\ell(t)$ and relative phase $\phi_{\ell+1/2}$ for a deep lattice ($\delta/U = 10^{-2}$) in the saturation regime ($T_p b/w \sim 7$). Upper panels: early stage ($t = 16\hbar/E_R$); lower panels: late stage ($t = 200\hbar/E_R$).

To demonstrate the saturation of the signal, we follow the evolution of the system for a long time and look at the amplitudes Δn and $\Delta\phi$. Both in the GPE (for relatively deep lattices) and in the DNL simulations, we find an interesting scaling law that helps to distinguish between the three regimes mentioned above and makes evident the saturation of the signal amplitude. The scaling of the results is shown in Fig.7: The effect of the perturbing potential takes a universal form when:

- the perturbation parameters are combined in the form $T_p b/w$ which reflects the capability of the system to react to an external perturbation;
- the relative density variation is rescaled as $\Delta n \sqrt{U/\delta}$, while the amplitude of the relative phase signal $\Delta\phi$ does not need to be rescaled.

The results summarized in Fig.7, show that for small parameter $T_p b/w$, the perturbation produced in the system is small, and depends linearly on $T_p b/w$. Increasing the perturbation parameter $T_p b/w$, the signal amplitude Δn quickly saturates. The three regions indicated in Fig.7 correspond to the three regimes (1-3) listed above.

From our numerical results, we find that the proportionality between the relative density and the relative

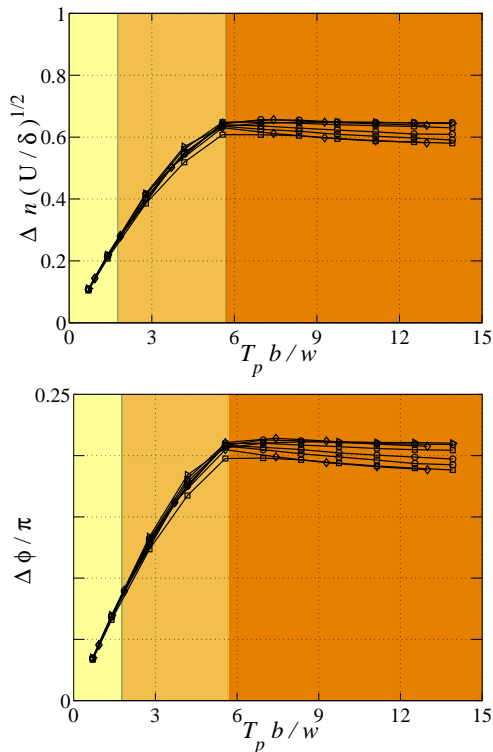


FIG. 7: Results for the density and relative signal amplitudes Δn and $\Delta\phi$ obtained from DNLS simulations for varying perturbation parameters T_p , b , w (see Eq.(3)), tunnel coupling δ and on-site interaction U (see Eq.(12)) with $\delta \ll U/3$.

phase amplitudes written in Eq.(16), holds also beyond the linear regime. In particular, we found a saturation of the relative phase amplitude at a value $\Delta\phi \approx 0.2\pi$, which goes with the saturation of the density amplitude Δn . This implies that for given interaction and lattice depth, the amplitude of the density signal is limited by approximately $\Delta n \approx 0.2\pi\sqrt{\delta/U}$.

Saturation does not occur in the uniform system or at low lattice depth. To demonstrate this, we plot in Fig. 8 the signal amplitude Δn measured after different propagation times for $s = 0$ (dashed lines) and $s = 15$ (solid lines) as a function of potential height b , with fixed potential width w and perturbation time T_p . With $s = 15$ the signal amplitude takes exactly the same values at $t = 100, 200, 300, 400\hbar/E_R$ (the corresponding four lines in Fig. 8 perfectly overlap!). In contrast, the signal amplitudes in the uniform system ($s = 0$, dashed lines) at different times ($t = 100, 200\hbar/E_R$) differ from each other: At earlier times the signal amplitude increases as a function of the strength of the external perturbation and does not saturate. The amplitude measured at later times coincides with the one measured earlier only for small potential heights b , when the propagation dynamics is linear. When nonlinear effects becomes important, Δn decreases during the evolution as a consequence of the dispersion of the signal.

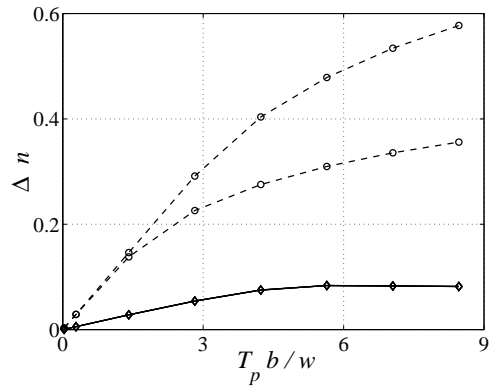


FIG. 8: The signal amplitude Δn as a function of the perturbation parameter bT_p/w at $gn = 0.5E_R$. Dashed lines: GP simulation for $s = 0$ and $gn = 0.5E_R$ at $t = 100\hbar/E_R$ (upper dashed line) and $t = 200\hbar/E_R$ (lower dashed line). Solid lines: GP simulation for $s = 15$ and $gn = 0.5E_R$ at $t = 100, 200, 300, 400\hbar/E_R$ for $s = 15$. The corresponding four lines exactly overlap.

V. ROLE OF HARMONIC TRAPPING

Realistic experimental setups include an harmonic trapping potential in the parallel and transverse directions of the lattice.

In the longitudinal direction, the harmonic trap has a negligible effect on sound propagation if $L \gg wd$, being L the size of the condensate and w the width of the perturbing potential. This condition guarantees, first of all, that the sound wavepacket travels in a region of approximately constant average density. Moreover it ensures that low energy discretised modes [15] are not strongly excited.

In the Thomas-Fermi regime, we find that the time required by the sound signal to travel along a distance of the order of the size of the condensate is $\sim 2\pi/\omega_D$, with $\omega_D = \sqrt{m/m^*}\omega_x$ the renormalised dipole frequency [24, 33].

The transverse harmonic trapping leads to an inhomogeneous radial density profile which can affect the sound velocity. Even in the uniform case, a radial Thomas-Fermi density distribution changes the sound velocity $c = \sqrt{U/m}$ to $c = \sqrt{U/2m}$ [12, 13, 14, 15]. The analogous modification of the velocity of sound to $c = \sqrt{U/2m^*}$ is expected in presence of the lattice provided the inverse compressibility U is linear in the density, as discussed in [28, 29, 30]. This approximation requires the interactions gn to be sufficiently small and has proven applicable to describe the experimental result on collective excitations [34] and on the condensate size [35] where $gn \approx 0.2 \div 0.5E_R$.

Moreover the predicted effects require single band dynamics. This is ensured if the radial trapping frequency is larger than the width of the first Bogoliubov band. In the tight binding regime, this condition reads $\hbar\omega_\perp > 2\sqrt{U\delta}$.

VI. CONCLUSIONS

In conclusion, we find that there exists a broad range of optical potential depths where the change in sound velocity induced by the lattice should be measurable also in the non linear regime. For instance, a velocity of propagation $c = 0.65c_{s=0}$ and $0.30c_{s=0}$ can be measured at an optical lattice depth of $s = 10$ and 20 with a maximal density variation $\Delta n_{\max} = 0.13$ and 0.05 respectively. This maximal attainable signal amplitude decreases very strongly with the optical lattice depth, making the signal in practise observable only up to a certain lattice depth which depends on the interaction strength.

We have shown that the presence of a deep lattice has a dramatic effect on the propagation of sound signals in the nonlinear regime: Contrary to the uniform system, shock waves propagate slower than sound waves, due to the

negative curvature of the dispersion relation in the lowest Bogoliubov band. Moreover, nonlinearities can play a role also at very small density variations and induce a saturation of the sound signal, which goes along with dephased currents left behind the signal. This effect has no analogue in the uniform case. One should also keep in mind, that the saturation effect is clearly evident only if the shock waves move with a velocity much lower than the sound velocity, which requires $\delta/U \ll 1/3$. Obtaining a clear saturation effect (small δ/U) associated with a large signal amplitude Δn (large δ/U) at fixed lattice depth requires a compromise in the choice of lattice depth s and interaction strength gn .

This research is partially supported by the Ministero dell'Istruzione, dell'Università e della Ricerca (MIUR), and by the U.S. Department of Energy through the Theoretical Division at the Los Alamos National Laboratory.

-
- [1] D. Jaksch, C. Bruder, J.I. Cirac, C.W. Gardiner and P. Zoller, Phys. Rev. Lett. **81**, 3108 (1998).
 - [2] M. Greiner, O. Mandel, T. Esslinger, T.W. Hänsch and I. Bloch, Nature **415**, 39 (2002).
 - [3] B. Wu and Q. Niu, Phys. Rev. A **64**, 061603 (2001).
 - [4] A. Smerzi, A. Trombettoni, P.G. Kevrekidis, and A.R. Bishop, Phys. Rev. Lett. **89**, 170402 (2002).
 - [5] C. Menotti, A. Smerzi, and A. Trombettoni, New J. Phys. **5**, 112 (2003).
 - [6] F.S. Cataliotti, L. Fallani, F. Ferlaino, C. Fort, P. Maddaloni, and M. Inguscio, New J. Phys. **5**, 71 (2003).
 - [7] F. Nesi and M. Modugno, cond-mat/0310659
 - [8] M. Cristiani, O. Morsch, N. Malossi, M. Jonas-Lasinio, M. Anderlini, E. Courtade, E. Arimondo, cond-mat/0311160
 - [9] S.L. Rolston and W.D. Phillips, Nature **416** 219, (2002) and refs therein.
 - [10] M. A. Kasevich, Science **298** 1363 (2002) and refs therein.
 - [11] M.R. Andrews, D.M. Kurn, H.-J. Miesner, D.S. Durfee, C.G. Townsend, S. Inouye, and W. Ketterle, Phys. Rev. Lett. **79**, 553 (1997).
 - [12] M.R. Andrews, D.M. Stamper-Kurn, H.-J. Miesner, D.S. Durfee, C.G. Townsend, S. Inouye, and W. Ketterle, Phys. Rev. Lett. **80**, 2967 (1998).
 - [13] E. Zaremba, Phys. Rev. A **57**, 518 (1998).
 - [14] G.M. Kavoulakis and C.J. Pethick, Phys. Rev. A, **58** 1563 (1998).
 - [15] S. Stringari, Phys. Rev. A **58**, 2385 (1998).
 - [16] B. Damski, cond-mat/0309421
 - [17] A.V. Gurevich and L.P. Pitaevskii, Sov. Phys. JETP **38**, 291 (1974).
 - [18] A.V. Gurevich and A.L. Krylov, Sov. Phys. JETP **65**, 944 (1987).
 - [19] The term *shock wave* is usually used to describe waves in presence of dissipation; the ones we refer to in this paper are oscillating structures which should be rather addressed as *collisionless shock waves*.
 - [20] K. Berg-Sørensen and K. Mølmer, Phys. Rev. A **58**, 1480 (1998).
 - [21] J. Javanainen, Phys. Rev. A **60**, 4902 (1999).
 - [22] M.L. Chiofalo, M. Polini and M.P. Tosi, Eur. Phys. J. D **11**, 371 (2000).
 - [23] D. van Oosten, P. van der Straten, and H. T. C. Stoof, Phys. Rev. A **63**, 053601 (2001).
 - [24] M. Krämer, L. Pitaevskii and S. Stringari, Phys. Rev. Lett. **88**, 180404 (2002).
 - [25] A.M. Rey, K. Burnett, R. Roth, M. Edwards, C.J. Williams, and C.W. Clark, J. Phys. B **36**, 825 (2003).
 - [26] M. Machholm, C.J. Pethick, and H. Smith, Phys. Rev. A **67**, 053613 (2003).
 - [27] E. Taylor and E. Zaremba, Phys. Rev. A **68**, 053611 (2003).
 - [28] A. Smerzi and A. Trombettoni, Phys. Rev. A **68**, 023613 (2003).
 - [29] M. Krämer, C. Menotti, L. Pitaevskii and S. Stringari, Eur. Phys. J. D **27**, 247 (2003).
 - [30] J.-P. Martikainen and H.T.C. Stoof, cond-mat/0308626
 - [31] A. Trombettoni and A. Smerzi, Phys. Rev. Lett. **86**, 2353 (2001).
 - [32] The exact sound velocity can be extracted in this way, thanks to our specific excitation method: a similar measurement performed on a bright (grey) sound signal would lead to a slightly higher (lower) value for the sound velocity.
 - [33] F.S. Cataliotti, S. Burger, C. Fort, P. Maddaloni, F. Minardi, A. Trombettoni, A. Smerzi, M. Inguscio, Science, **293** 843 (2001).
 - [34] C. Fort, F.S. Cataliotti, L. Fallani, F. Ferlaino, P. Maddaloni, and M. Inguscio, Phys. Rev. Lett. **90**, 140405 (2003).
 - [35] O. Morsch, M. Cristiani, J.H. Müller, D. Ciampini and E. Arimondo, Phys. Rev. A **66**, 021601 (2002).